

## INTRODUCTION

In recent years, advances in tissue engineering techniques have allowed for micro-patterning of cardiac cells in engineered monolayers with controlled anisotropy, fiber direction and spacing. These techniques are a valuable tool that can be used to *observe* the effect of cellular properties (orientation, connectivity, etc) on cardiac conduction. However, there are inherent limitations in experimental preparations that limit the ability to understand the *role* of cellular structure on propagation, and the use of computational simulations has allowed for numerous insights into the electrophysiological properties of cardiac tissue that are not possible through experimental preparations alone.

Simulations of discrete cardiac tissue can incorporate cellular level detail, but these simulations are computationally difficult and time-consuming; instead, continuous bidomain simulations can provide similar levels of insight while significantly simplifying the computational load of each problem. The continuous model requires as parameters the effective intracellular and extracellular conductivities of the tissue which are homogenized values that are affected by the tissue geometry, coupling, and many other physical factors that are difficult to determine experimentally.

We demonstrate a novel method for estimating effective intracellular conductivities in cardiac monolayers by considering the transmembrane potential distributions following a long-duration hyperpolarizing stimulation and fitting a continuous model to experimental data to estimate effective conductivities with less than 10% error. Estimating these conductivity values will allow us to determine the functional consequences of certain interventions that affect structure and to develop computational models to help elucidate the mechanisms of conduction failure.

## COMPUTATIONAL METHODS

### The Continuous Bidomain Model

The continuous model of cardiac tissue represents the tissue as two coupled homogenous domains connected by a membrane. Our continuous model provides an estimation of the voltage distribution given a intracellular conductivity tensor  $\mathbf{g}_i = (g_{ix}, g_{iy})$

**State Variables**  
 $\phi_e$  : Extracellular potential       $\phi_i$  : Intracellular potential

### Domain and Boundary Conditions:

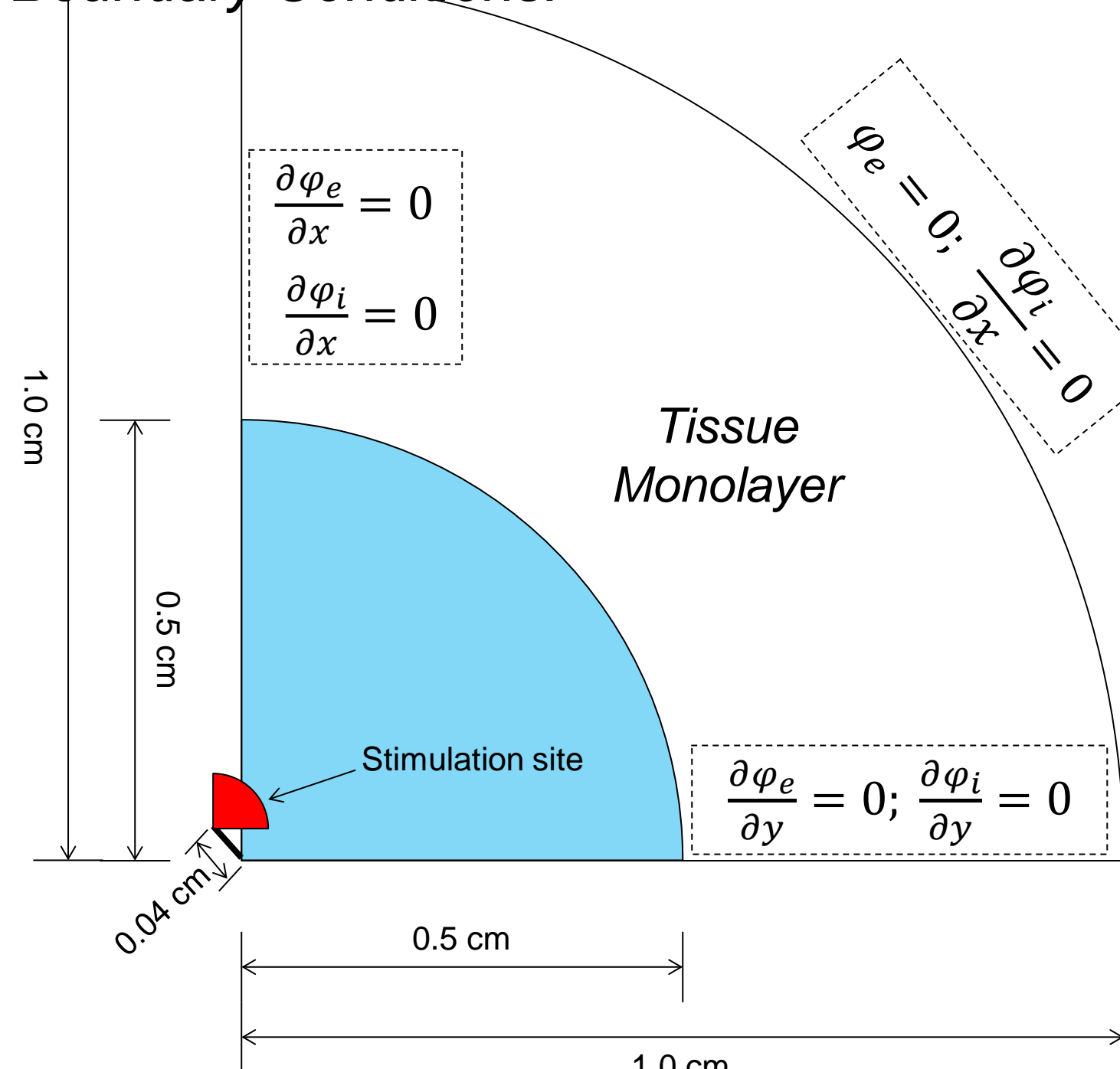


Figure 1. Domain and boundary conditions for continuous model

### Governing Equations:

$$\begin{aligned} \nabla \cdot (\mathbf{g}_i \nabla \phi_i) &= \beta I_m \\ \nabla \cdot (\mathbf{g}_e \nabla \phi_e) &= -\beta I_m - \beta I_{stim} \\ V_m &= \phi_i - \phi_e \end{aligned}$$

Where  $I_m = I_m(V_m)$  is the sum of the capacitive and ionic currents,  $\mathbf{g}_i$  is the tensor of bidomain intracellular conductivities,  $\mathbf{g}_e$  is the scalar value of bidomain conductivity in the isotropic extracellular space,  $\beta$  is the surface area to volume ratio for each cell,  $V_m$  is the transmembrane potential, and  $I_{stim}$  is the applied extracellular stimulus current

The governing equations were solved over the domain using the FlexPDE finite element method package. The package utilizes adaptive mesh and timestep techniques to efficiently generate an accurate solution. Extracellular conductivities were assumed to be fixed at literature values of  $(g_{ex}, g_{ey}) = (3.0, 1.9)$  mS/cm

### The Augmented Monodomain Formulation for Bath Stimulation of Monolayers

The addition of a large bath to the bidomain model significantly increases the computational load involved in solving the system. In order to maintain the ability to perform bath stimulation while reducing the computational intensity of the simulation, we developed a novel augmented monodomain model for bath stimulation that applies the concept of the activating function that is commonly used in neural electrophysiology.

In the bath region of the bidomain model, the extracellular voltage is the primary variable of interest while in the cell layer itself, the intracellular potential plays a relatively dominant role in determining the steady state transmembrane potential, with the extracellular potential providing the driving force during stimulation. We can therefore decouple the bath from the tissue layer and consider the two regions separately.

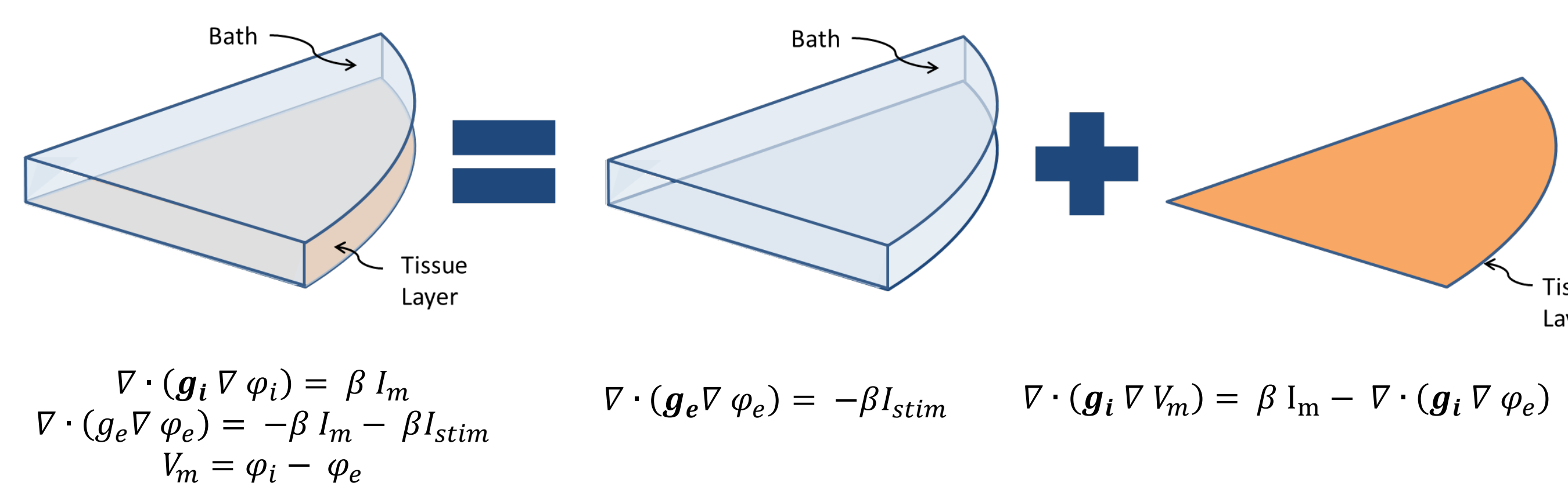


Figure 2. Decoupling of the bath and tissue layer domains

### Simplifying the Membrane

Preliminary evidence from our group suggested that membrane resistance was not constant during subthreshold stimulation. Therefore, the membrane resistance was modeled as a function of membrane potential, approximately fitting data from the Pandit membrane model.[1]

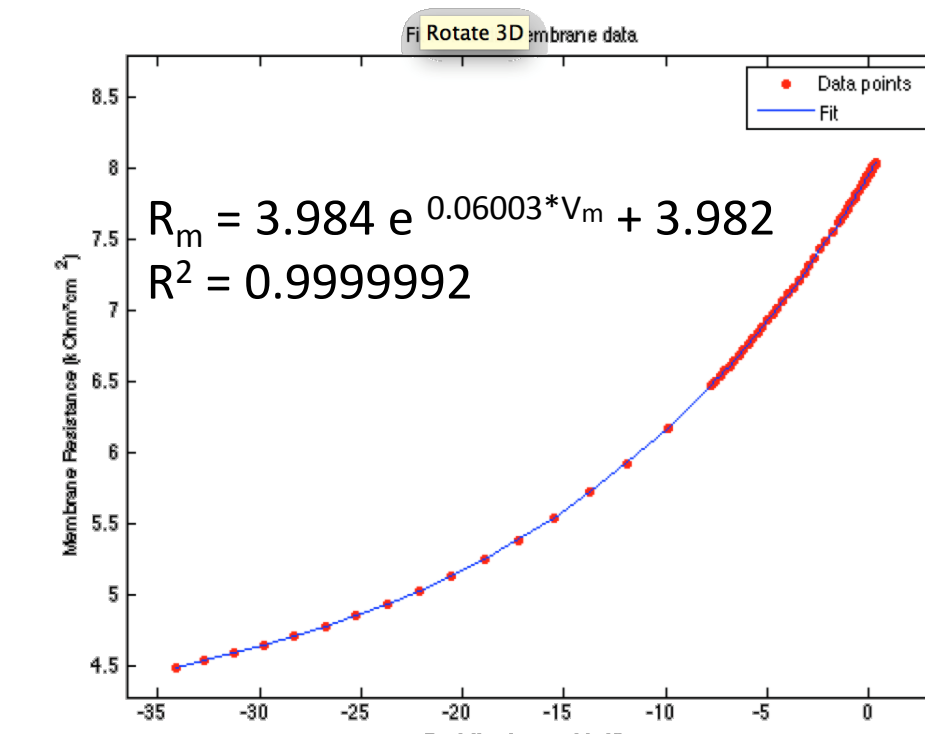


Figure 3. Membrane resistance as a function of membrane potential for the Pandit membrane model, and its functional approximation

### Generation of Surrogate Data from Discrete Model

In order to test our estimation system, surrogate experimental data was generated from a discrete model of cardiac tissue that models individual cells and the gap junctions connecting them. The benefit of surrogate data from a discrete model is that the effects of individual cells and their properties are incorporated as in experimental preparations, but the "ground truth" conductivities can be mathematically determined to compare to the estimated values.

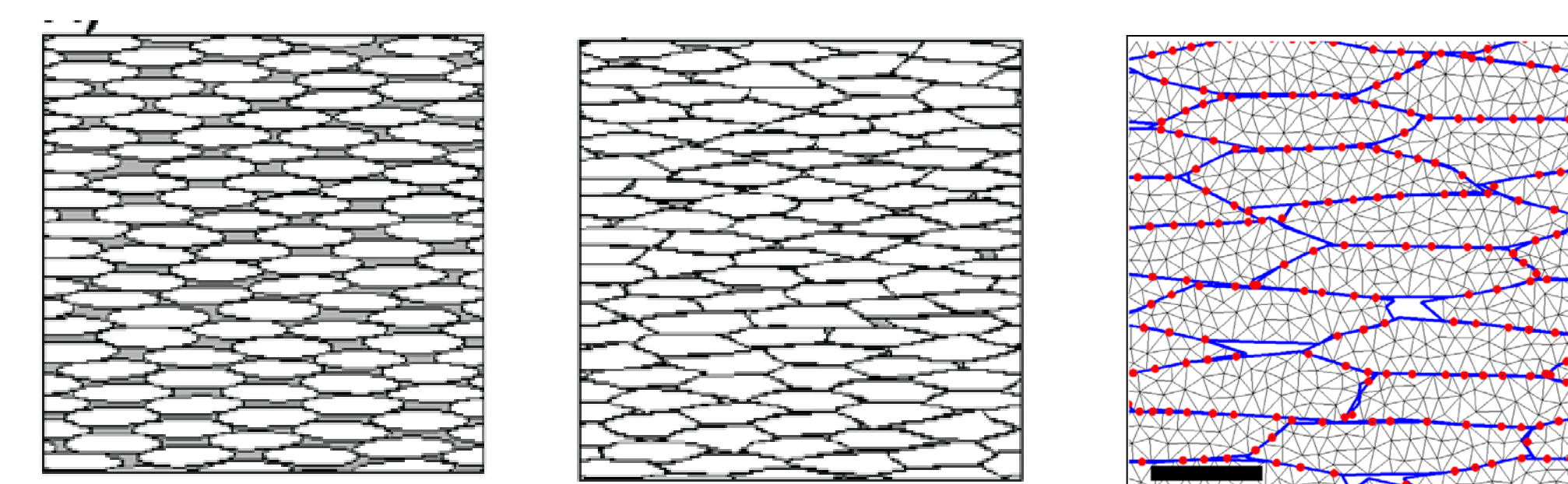


Figure 4. To generate discrete tissue models, oval template cells are laid over the domain and then expanded to fill the domain. Gap junctions are identified at neighboring cells and the cells are then divided into elements for finite element calculations. The tissue generator allows for adjustment of cellular anisotropy and cellular cleft spacing [2]

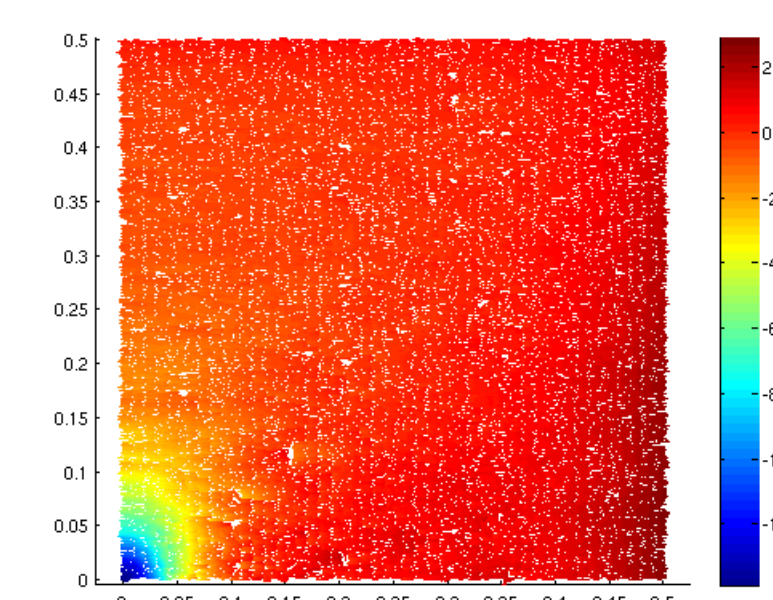


Figure 5. A sample voltage distribution following hyperpolarizing stimulation of the discrete model. The Pandit membrane model was used to generate surrogate data

### Parameter Estimation

In order to determine the conductivity tensor  $\mathbf{g}_i$  that best estimates the bidomain conductivities of the known tissue, an error function was defined. All data were first spatially averaged over 135 circular regions to simulate the format in which voltage distribution data from experimental preparations would be recorded. The error was then defined as

$$E(\mathbf{g}_i) = \frac{1}{N} \sum_i (V_i^{true} - V_i^{sim}(\mathbf{g}_i))^2$$

where N is the number of sensors,  $V_i^{true}$  is the experimental or known transmembrane voltage from the  $i^{th}$  sensor, and  $V_i^{sim}(\mathbf{g}_i)$  is the transmembrane voltage from it  $i^{th}$  sensor, using conductivity tensor  $\mathbf{g}_i$

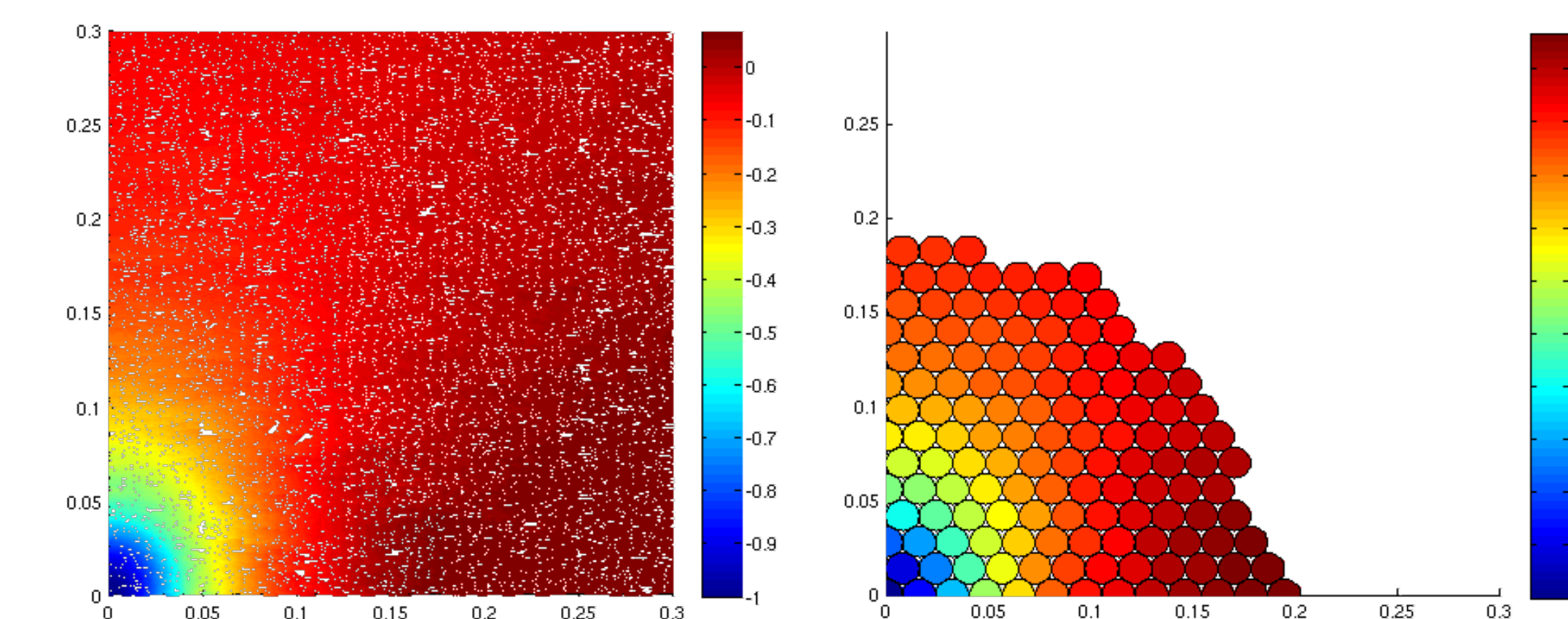


Figure 6. Sample surrogate data (left) and corresponding spatially averaged data (right)

An technique was then developed to find the conductivity tensor that minimizes the error function. A differential evolution algorithm as described by Storn et al. was coupled with the continuous model simulation and error calculation steps. [3]

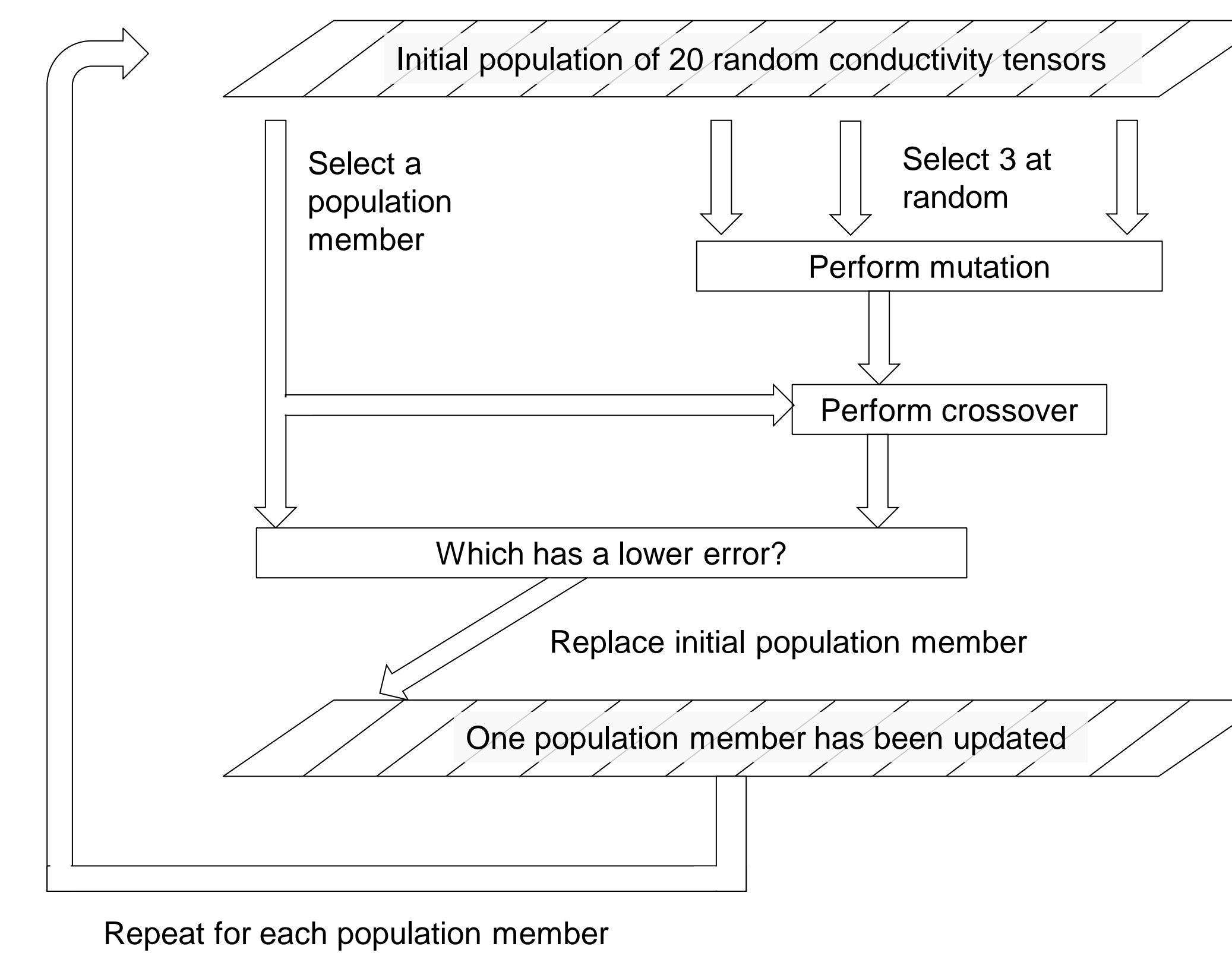


Figure 7. Illustration of one generation of Differential Evolution algorithm. This process is repeated until the maximal generations are reached or the minimum error threshold is reached

## RESULTS

### Validating the augmented monodomain formulation

We validated the augmented monodomain formulation for bath stimulation of monolayers by comparing results of the continuous true bidomain with the continuous augmented monodomain over a variety of conductivities.

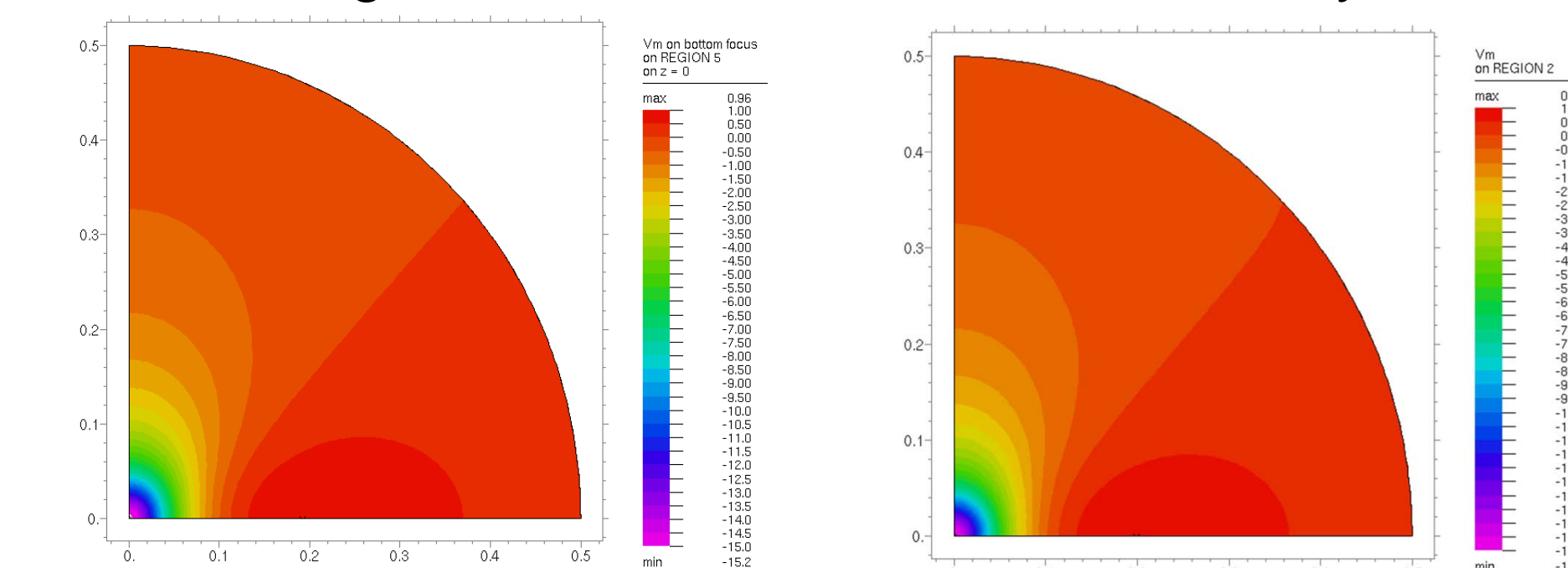


Figure 8. Sample comparison of distributions from true bidomain (left) and augmented monodomain (right) shows no difference in result but the augmented monodomain significantly reduces computational load for multiple runs

### Validating the estimation method

We validated the estimation method by generating surrogate data using a continuous model with known intracellular conductivity values. We then performed spatial averaging of this data as previously described and used it in place of the experimental data in the error formula. The Differential Evolution algorithm provided consistently accurate estimations of the intracellular conductivity values.  $g_{ix}$  was estimated with an average of 0.6% error and  $g_{iy}$  was estimated with an average of 1.05% error.

### Estimation of Conductivities from Surrogate Data

Cases over a wide range of conductivity values and anisotropy ratios were tested. In relatively anisotropic surrogate tissues, the conductivities were estimated with an average 5.25% error ( $\pm 2.26\%$ ) along the principal axis of anisotropy and an average 9.92% error ( $\pm 6.83\%$ ) perpendicular to the principal axis of anisotropy. In relatively isotropic tissues, the conductivities were estimated with an average error of

Known Conductivities	Estimated Conductivities
$g_{ix} = 2.302$ mS/cm	$g_{ix} = 2.4254 \pm 0.00012$ mS/cm
$g_{iy} = 0.246$ mS/cm	$g_{iy} = 0.2428 \pm 0.00004$ mS/cm
$g_{ix} = 1.487$ mS/cm	$g_{ix} = 1.5754 \pm 0.00012$ mS/cm
$g_{iy} = 0.203$ mS/cm	$g_{iy} = 0.1839 \pm 0.00005$ mS/cm
$g_{ix} = 1.591$ mS/cm	$g_{ix} = 1.5561 \pm 0.00005$ mS/cm
$g_{iy} = 0.188$ mS/cm	$g_{iy} = 0.1543 \pm 0.00001$ mS/cm

Table 1. Several examples of known and estimated conductivities are shown

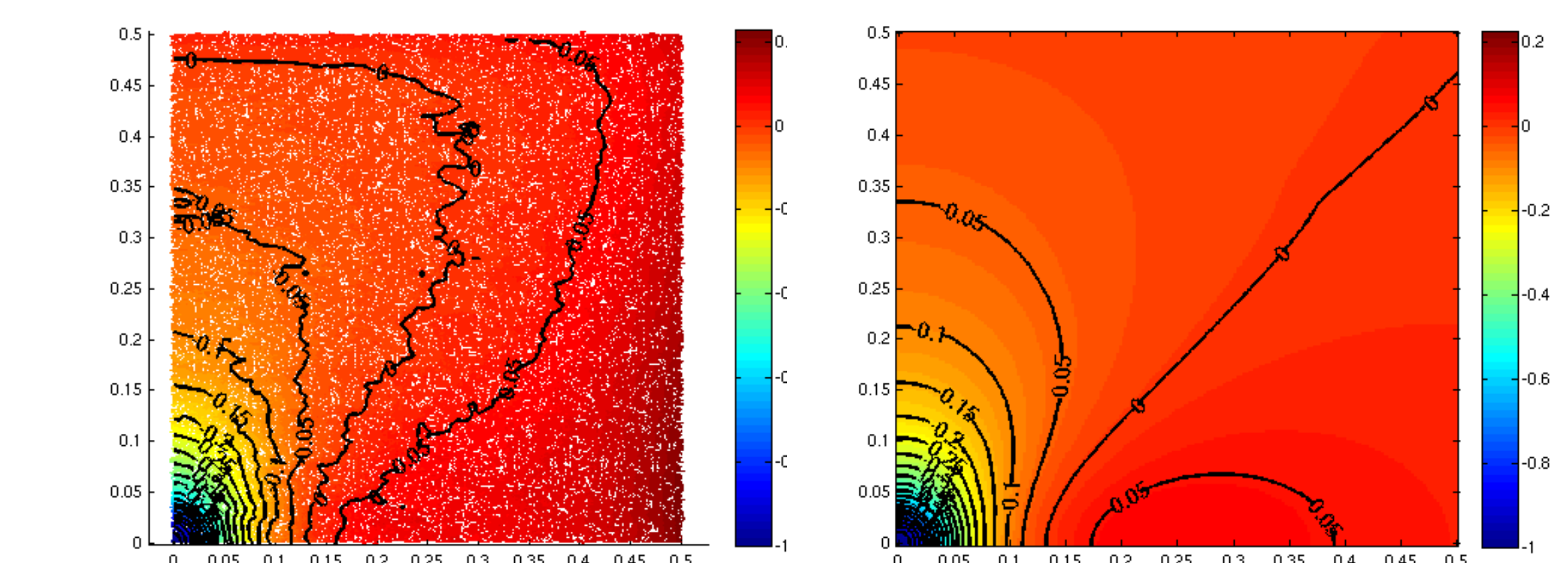


Figure 9. Sample comparison of contours from surrogate data (left) and continuous model with estimated conductivities (right) in an anisotropic tissue. For this example, error in estimates was 5.36% along axis of anisotropy and 1.31% perpendicular to axis

## CONCLUSIONS AND FUTURE WORK

We have demonstrated the ability to use our spatially averaged error calculation and differential evolution method to estimate intracellular conductivity values with less than 10% error, using surrogate data from a discrete model whose conductivities can be measured.

Our preliminary data suggests that as tissues become more anisotropic, accuracy of estimates along the principal axis of anisotropy increases and accuracy perpendicular to the principal axis decreases.

We plan to use this method to estimate conductivities of tissue engineered (experimental) monolayers by measuring potentials using a voltage sensitive optical dye. These resulting estimated conductivities will be used to generate continuous models of cardiac tissue that replicate the properties of the tissue engineered monolayers.

We will also use this method to measure the bulk conductivity properties of discrete tissues, which will allow us to examine how micro-structural changes in our tissue affect conduction in the bulk tissue.

## ACKNOWLEDGEMENTS

This work was supported by National Institutes of Health Grant HL093711-01A2 to C.H. and the MSTP Training Grant T32-GM007171. Special thanks to Dr. Letitia Hubbard and Shravan Verma for their assistance

## REFERENCES

- [1] Pandit SV et al. *Biophysical Journal*. ,2001; 81, 3029-3051.
- [2] Kim JM, Bursac N, Henriquez CS.. *Biophysical journal*. 2010;98(9):1762-71
- [3] Storn R, Price K. *Journal of global optimization*. 1997;11(4):341-359.

## CONTACT

Tanmay Gokhale  
 MD-PhD Student  
 Department of Biomedical Engineering  
 tanmay.gokhale@duke.edu